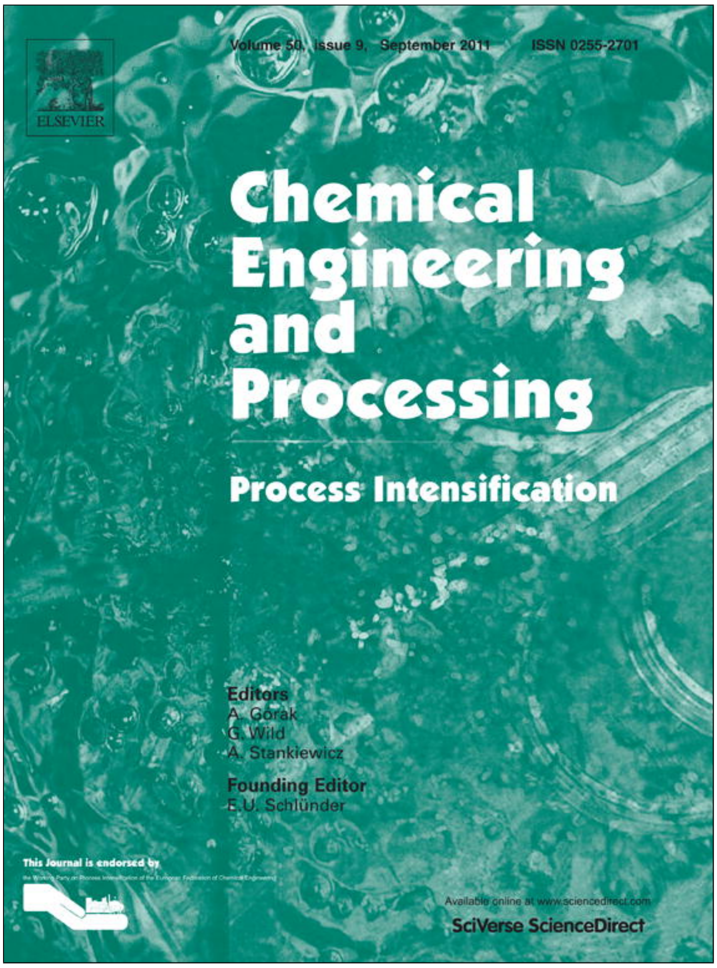
Volume 50, Issue 9, September 2011 ISSN 0255-2701
ELSEVIER
Chemical Engineering and Processing
Process Intensification
Editors
A. Górak
G. Wild
A. Stankiewicz
Founding Editor
E.U. Schlünder
This Journal is endorsed by
Available online at www.sciencedirect.com
SciVerse ScienceDirect

Chemical Engineering and Processing 50 (2011) 940–943

Contents lists available at ScienceDirect

Chemical Engineering and Processing: Process Intensification

journal homepage: www.elsevier.com/locate/cep

Mass-transfer studies at rotating cylinder electrodes with turbulence promoters

J.M. Grau, J.M. Bisang*

Programa de Electroquímica Aplicada e Ingeniería Electroquímica (PRELINE), Facultad de Ingeniería Química, Universidad Nacional del Litoral, Santiago del Estero 2829, S3000 AOM Santa Fe, Argentina

ARTICLE INFO

Article history:
Received 13 December 2010
Received in revised form 5 July 2011
Accepted 7 July 2011
Available online 18 July 2011

Keywords:
Electrochemical reactors
Mass-transfer
Rotating cylinder electrode
Turbulence promoter

ABSTRACT

Mass transfer was studied at a rotating cylinder electrode with different turbulence promoters using the reduction of ferricyanide as a test reaction. Four types of turbulence promoters were examined: expanded plastic meshes, Teflon structures, a plastic woven mesh and a plastic perforated net, which were rotated together with the electrode. The best performance was obtained for the Teflon structures at low rotation speeds and for the plastic woven mesh at high rotation speeds. The effect of both the length and the number of sheets of the turbulence promoters as well as the use of static promoters were also analysed. Comparisons of mass-transfer performance of turbulence promoters are made with other three-dimensional structures. The mass-transfer enhancement factor related to a smooth rotating cylinder electrode is twice as large.

1. Introduction

The performance of electrochemical reactors can be enhanced by the use of flow obstacles in the interelectrode gap to promote turbulence [1]. Thus, Cœuret and Storck [2] summarized mass-transfer correlations for different turbulence promoters. Also, the rotating cylinder electrode, whose good mass-transfer conditions are achieved by the movement of the electrode, has been recognized as a helpful tool in applied electrochemistry [3]. Besides, the incorporation of electroactive turbulence promoters has been suggested to further increase the space time yield. Hence, Kappesser et al. [4] performed some mass-transfer research at rotating cylinders with staggered diamond knurls machined on their surfaces. Sedahmed et al. [5] studied mass-transfer at rotating finned cylinders, where fins were made by cutting longitudinal rectangular grooves in the cylinder. Makanjuola and Gabe [6] reported mass-transfer studies at V-grooved cylinders and the research was extended to pyramidal knurling and wires or meshes wound to the cylindrical rotating electrode [7]. Further mass-transfer studies at rotating cylinder electrodes in terms of the roughness factor are discussed by Gabe et al. [8]. Furthermore, the introduction of baffles in the electrochemical cell has little effect on the behaviour of a reticulated vitreous carbon rotating cylinder electrode, and a jet electrolyte flow towards the electrode can enhance the mass-transfer rate by a factor ranging from 1.03 to 1.46, depending on the electrode type [9].

The latest research works show that the enhancement of the reactor performance is attributed to the concurrent increase of the mass-transfer coefficient and to the specific surface area of the electrode. The aim of the present work is to quantify the isolated effect of turbulence promoters on mass-transfer in rotating cylinder electrodes and to compare mass-transfer characteristics with similar rotating structures.

2. Experimental

The experiments were performed in an undivided batch reactor (95 mm int. dia. and 140 mm high) maintained at a constant temperature by a heating jacket. Fig. 1 shows the configuration of the electrochemical reactor. The working electrode was a nickel rotating cylinder, 26.6 mm diameter, 80 mm long and 66.8 cm^2 electrode surface area. The surface of the working electrode was polished to a bright mirror finish with slurry of 0.3 μm alumina powder and it was washed with acetone in an ultrasonic cleaner. The upper end of the cylinder was attached to the motor shaft. A brass disc, centrally positioned, was used as electric contact for the electrode, whose lower end was closed with a Teflon disc. The turbulence promoter was wound around the rotating cylinder. Four types of turbulence promoters were used: expanded plastic meshes, Teflon structures, a plastic woven mesh and a plastic perforated net. The Teflon structures present a similar configuration to that of the expanded plastic meshes, but with a greater variation in their dimensions. The Teflon structures were produced by making axial cuts in a thermosetting Teflon tube, expanding the tube with a cylinder of a larger

* Corresponding author. Tel.: +54 342 4571164 (2608); fax: +54 342 4571164 (2535).
E-mail address: jbisang@fiq.unl.edu.ar (J.M. Bisang).

0255-2701/$ – see front matter © 2011 Elsevier B.V. All rights reserved.
doi:10.1016/j.cep.2011.07.006

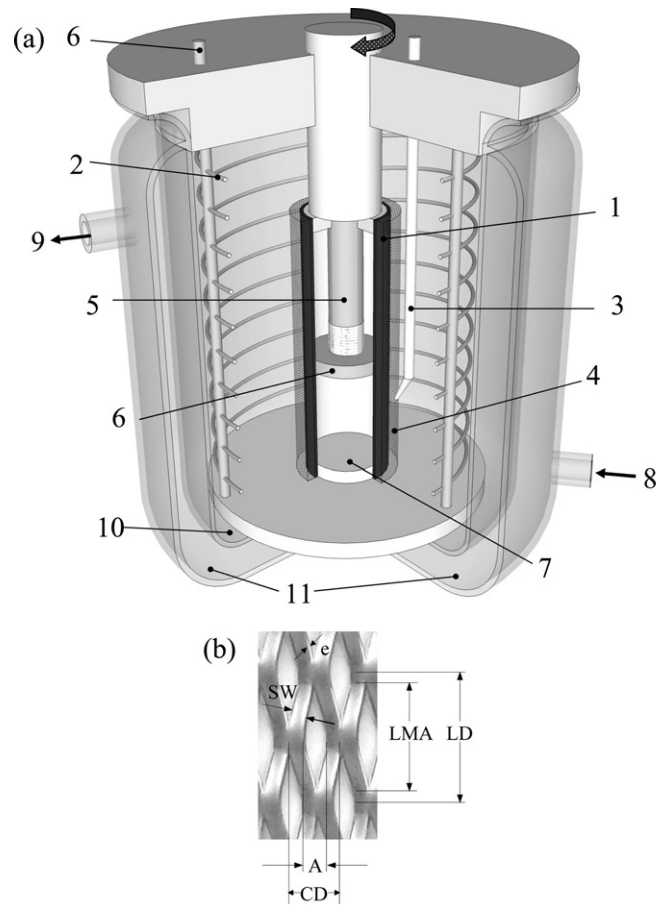

Fig. 1. (a) Exploded view of the electrochemical reactor. (1) working electrode, (2) counterelectrode, (3) Luggin capillary, (4) turbulence promoter, (5) electrode shaft, (6) electric contact, (7) Teflon disc, (8) water inlet, (9) water outlet, (10) container for holding electrolyte and (11) heating jacket. (b) View of the expanded plastic with the characteristic parameters according to Table 1.

diameter and fixing the configuration by heating. The geometrical characteristics, measured in the laboratory and defined in Fig. 1(b), are summarized in Table 1. The turbulence promoter was rotated together with the electrode, but in some experiments it was maintained static with respect to the rotating electrode at a different distance each time. A helical nickel wire (1.5 mm dia. × 190 cm long) with an interelectrode gap of 24 mm was used as counterelectrode. The working electrode and the counterelectrode were concentric, thereby ensuring a uniform primary current distribution. The reference electrode was a saturated calomel electrode and the potential was controlled against the reference electrode connected to a Luggin capillary placed in the middle of the rotating electrode.

Table 1
Geometrical parameters of the turbulence promoters.

Characteristic parameters of the expanded plastics	○	♦	●	△
Long diagonal (LD/mm)	6.7	14.3	16.2	21.0
Short diagonal (CD/mm)	2.5	4.1	11.5	5.5
Long mesh aperture (LMA/mm)	3.2	9.5	11.0	12.5
Short mesh aperture (*A*/mm)	2.0	3.4	9.5	3.0
Thickness (*e*/mm)	0.2	0.9	0.5	1.2
Apparent thickness (e_a (1 sheet)/mm)	0.4	1.2	1.2	2.4
Strand width (SW/mm)	0.25	0.7	1.0	1.8

Characteristic parameters of the Teflon structures	▲	▽	◊
Long diagonal (LD/mm)	18	28	24
Short diagonal (CD/mm)	9	10	18
Long mesh aperture (LMA/mm)	13.5	24	20
Short mesh aperture (*A*/mm)	7	8	12
Thickness (*e*/mm)	0.6	0.6	0.6
Apparent thickness (e_a (1 sheet)/mm)	2.2	4.0	8.0
Strand width (SW/mm)	2.0	3.0	5.0

Characteristic parameters of woven and perforated meshes	+ (perforated net)	× (woven mesh)
Thread diameter (mm)	1.0	0.35
Distance between threads (mm)	1.3	1.1

Table 2
Properties of the electrolyte.

Composition	$[K_3Fe(CN)_6] = 1 \times 10^{-2}$ M $[K_4Fe(CN)_6] = 1 \times 10^{-2}$ M [NaOH] = 1 M
Density (kg m^{-3})	1.05×10^3
Dynamic viscosity (kg m^{-1} s^{-1})	1.12×10^{-3}
Kinematic viscosity (m^2 s^{-1})	1.07×10^{-6}
Diffusion coefficient (m^2 s^{-1})	6.09×10^{-10}
Sc	1757

The test reaction was the electrochemical reduction of ferricyanide from solutions with $[K_3Fe(CN)_6] \cong 1 \times 10^{-2}$ M, $[K_4Fe(CN)_6] \cong 1 \times 10^{-2}$ M, in 1 M NaOH as supporting electrolyte, while the reverse reaction occurred at the anode. Table 2 summarizes the composition and physicochemical properties of the solution. The cathode potential was swept from the open circuit potential (typically 200 mV vs SCE) to a value of −200 mV vs SCE and the current against potential curve was then recorded at a sweep rate of 1 mV s^{-1}. A well-defined limiting current was observed in all cases. Samples of the solution were taken from the reactor after each experiment and the ferricyanide concentration was spectrophotometrically determined using a Perkin-Elmer model Lambda 20 double-beam UV-Vis Spectrophotometer with 10 mm glass absorption cells and the supporting electrolyte was used as blank. The measurements were performed at a wavelength of 420 nm, where it is possible to determine the ferricyanide concentration without any interference of ferrocyanide. In a set of experiments, the above procedure was repeated for seven values of rotation speed in a given electrolyte. The experiments were performed at 30 °C and nitrogen was bubbled in the reactor for 1 h prior to the experiment in order to remove the dissolved oxygen.

The mass-transfer coefficient was calculated from the limiting current and the reactant concentration using the following equation [10]

$$k_m = \frac{I_{\text{lim}}}{\nu_e F S c} \tag{1}$$

where I_{lim} (A) is the limiting current, S (m^2) is the electrode surface area, c (mol m^{-3}) is the concentration of the electroactive species, ν_e is the number of electrons interchanged and F (96,485 C mol^{-1}) is the Faraday constant.

3. Results and discussion

Fig. 2 shows the mass-transfer coefficient for the four types of turbulence promoters as a function of rotation speed, ω (s^{-1}). The experimental mass-transfer coefficients for a smooth rotating cylinder electrode are also reported in this figure, which provides a baseline for performance comparison. The experimental values for a smooth rotating cylinder corroborate the classical mass-transfer correlation of Eisenberg et al. [11]. According to Fig. 2(a), the behaviour of expanded plastic meshes is comparable for the four types of studied structures in spite of the important differences in their geometrical parameters. However, a different performance is observed for a woven mesh and for a perforated net as turbulence promoters. Fig. 2(b) shows that all the turbulence promoters made

Table 3
Summary of correlation parameters.

	k_m = constant ω^a				
	Smooth electrode	Expanded plastic	Teflon structure	Woven mesh	Perforated net
Constant	1.809×10^{-6}	3.195×10^{-6}	4.475×10^{-6}	2.272×10^{-6}	2.087×10^{-6}
a	0.704	0.707	0.650	0.814	0.786

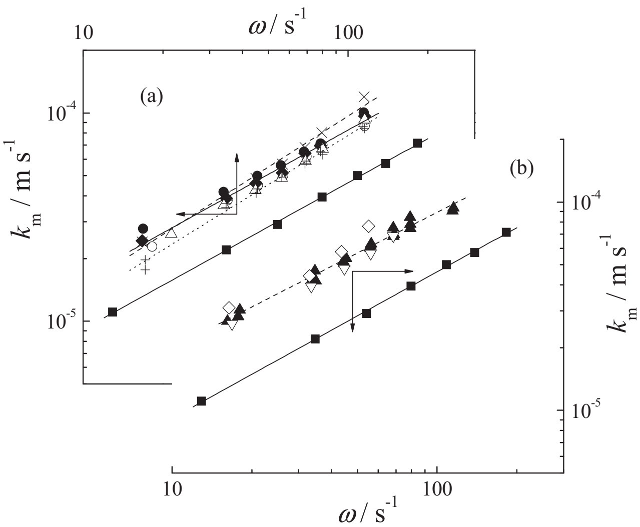

Fig. 2. Mass-transfer coefficient as a function of rotation speed. (a) Expanded plastics, woven mesh and perforated net as turbulence promoters. Full line: linear correlation for expanded plastics. Dashed line: linear correlation for woven mesh. Dotted line: linear correlation for perforated net. (b) Teflon structures as turbulence promoters. Dashed line: linear correlation. Full lines with (■): smooth rotating cylinder. Symbols according to Table 1.

with Teflon tubes present a similar behaviour. Table 3 summarizes the correlation parameters of the experimental results whose fitting lines are given in Fig. 2. The mass-transfer enhancement factor, which relates the mass-transfer coefficient in the presence of a turbulence promoter to the value of the smooth electrode, is reported in Fig. 3 in terms of the rotation speed, where the enhancement factor is approximately two for all the examined turbulence promoters. However, the best performance is obtained using either Teflon structures or woven meshes as turbulence promoters at low and high rotation speeds, respectively. Thus, for a woven mesh acting as a turbulence promoter the highest mass-transfer enhancement factor was 2.12 at a rotation speed of 115 s^{-1}. Similar values of the enhancement factor, ranging from 1.9 to 2.2, were noticed for wedge wire screens [12] or reticulated vitreous carbon [13]. However, for three-dimensional rotating cylinder electrodes of expanded metal [14] or woven-wire meshes [15], the mass-transfer coefficient is about three times higher than the ones obtained from a smooth electrode. The high value of the mass-

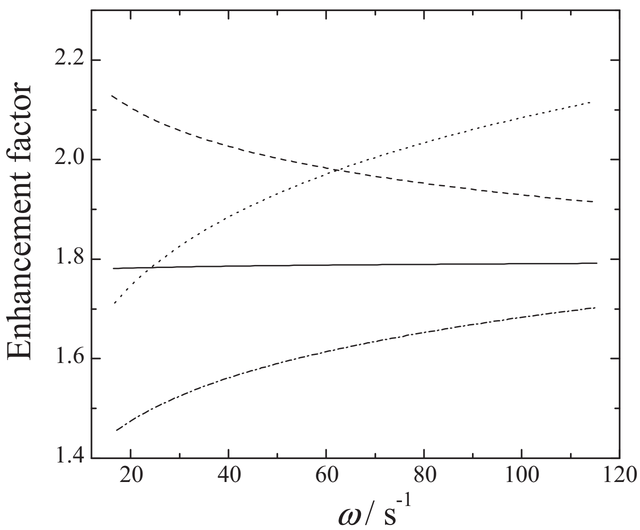

Fig. 3. Enhancement factor as a function of rotation speed. Full line: expanded plastics. Dashed line: Teflon structures. Dotted line: woven mesh. Dashed-dotted line: perforated net.

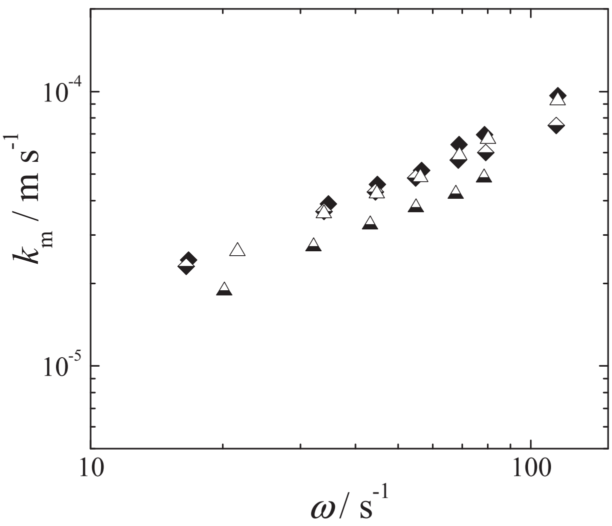

Fig. 4. Effect of the number of meshes of a turbulence promoter on the mass-transfer coefficient as a function of rotation speed. The symbols (♦) and (△) correspond to Table 1. The symbols partially filled represent the cases of two meshes, respectively.

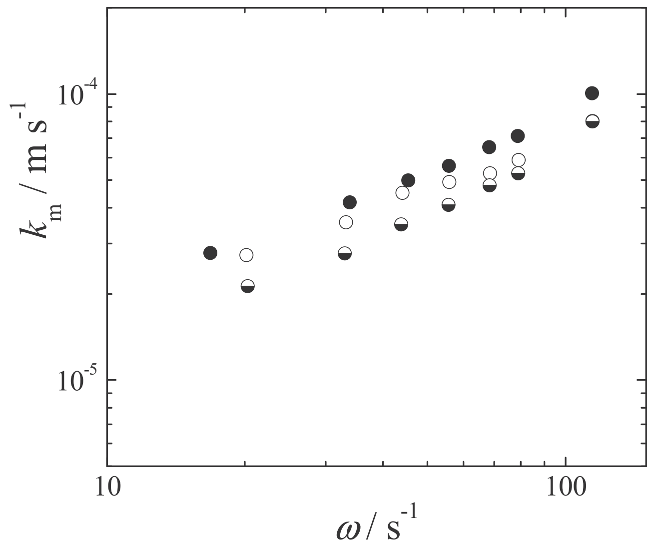

Fig. 5. Effect of the length of a turbulence promoter on the mass-transfer coefficient as a function of rotation speed. The symbol (●) corresponds to Table 1. Open circle: turbulence promoter placed at the electrode ends. Partially filled circle: turbulence promoter in the central part.

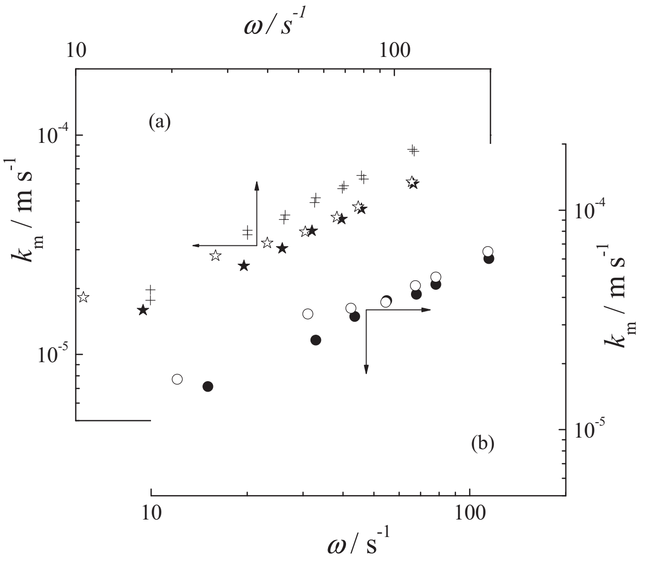

Fig. 6. Effect of the rotation and distance between the turbulence promoter to the rotating cylinder on the mass-transfer coefficient as a function of rotation speed. (a) Perforated net as turbulence promoter. The symbol (+) corresponds to Table 1 and the turbulence promoter is rotated together with the electrode. The stars correspond to a static perforated net as a turbulence promoter. (★) Distance 6.7 mm; (☆) distance 1.7 mm. (b) Static expanded metal coated with epoxy resin as a turbulence promoter. (●) Distance 6.7 mm; (○) distance 1.7 mm.

transfer enhancement factor for these electrodes can be attributed to the fact that the electrolyte flow was oriented through the sheet pack.

Fig. 4 compares the effect of the number of sheets of expanded plastic as turbulence promoters on the mass-transfer coefficient. The symbols (⧫) and (△) correspond to the experimental results reported in Fig. 2, where one mesh was used. The partially filled symbols represent two meshes of the same dimensions, respectively. It can be observed that the mass-transfer coefficient decreases when the number of meshes is doubled, which can be attributed to the shielding effect of the turbulence promoter.

Fig. 5 shows the influence of the length of expanded plastic as turbulence promoter. The symbol (●) corresponds to the case reported in Fig. 2. The open circles represent the same turbulence promoter separated into two parts and placed at the ends of the rotating cylinder, whereas the central part works without a turbulence promoter. The opposite case is represented by the partially filled circles. It is concluded that the mass-transfer characteristics diminish when the turbulence promoter does not cover the total electrode surface.

Fig. 6 compares the mass-transfer coefficient when the turbulence promoters are rotated together with the electrode or when they are static. For static promoters, two distances from the rotating cylinder were examined, i.e., 1.7 mm and 6.7 mm. Part (a) in Fig. 6 corresponds to the case of a perforated net as a turbulence promoter. It can be observed that in the case of static turbulence promoters, mass-transfer conditions diminish. A similar value in the mass-transfer coefficient is only obtained at low rotation speeds and when the static turbulence promoter is close to the rotating cylinder. Part (b) in Fig. 6 corresponds to an expanded metal, coated with epoxy resin, used as a turbulence promoter. A similar situation with the previous case is observed.

4. Conclusions

(i) Mass-transfer coefficients for rotating cylinder electrodes with turbulence promoters are, in general, twice as large as those obtained with smooth electrodes.
(ii) The influence of the geometrical parameters as well as the type of promoter was of little importance in mass-transfer behaviour for the examined promoters.
(iii) Woven meshes as turbulence promoters showed the best performance at higher rotation speeds, at 115 s^{-1} a mass-transfer enhancement factor of 2.12 was obtained. At rotation speeds lower than 60 s^{-1} Teflon structures, with geometric dimensions more pronounced than expanded plastic meshes, presented an appropriate behaviour.
(iv) The increase in the number of sheets of a turbulence promoter, the use of static promoters and the employment of a rotating cylinder partially covered with a promoter diminished the mass-transfer performance.

Acknowledgements

This work was supported by the Agencia Nacional de Promoción Científica y Tecnológica (ANPCyT), Consejo Nacional de Investigaciones Científicas y Técnicas (CONICET) and Universidad Nacional del Litoral (UNL) of Argentina.

References

[1] D. Pletcher, F.C. Walsh, Industrial Electrochemistry, Chapman and Hall, London, 1993, p. 344 (Chapter 7).
[2] F. Cœuret, A. Storck, Elements de Genie Electrochimique, TEC&DOC, Paris, 1984, pp. 148–155 (Chapter 3b).
[3] C.T. John Low, C. Ponce de Leon, F.C. Walsh, The rotating cylinder electrode (RCE) and its application to the electrodeposition of metals, Aust. J. Chem. 58 (2005) 246.
[4] R. Kappesser, I. Cornet, R. Greif, Mass transfer to a rough rotating cylinder, J. Electrochem. Soc. 118 (1971) 1957–1959.
[5] G.H. Sedahmed, A. Abdel Khalik, A.M. Abdallah, M.M. Farahat, Mass transfer at rotating finned cylinders, J. Appl. Electrochem. 9 (1979) 563–566.
[6] P.A. Makanjuola, D.R. Gabe, A study of roughness and mass transfer enhancement for the rotating cylinder electrode, Surf. Technol. 24 (1985) 29–44.
[7] D.R. Gabe, P.A. Makanjuola, Enhanced mass transfer using roughened rotating cylinder electrodes in turbulent flow, J. Appl. Electrochem. 17 (1987) 370–384.
[8] D.R. Gabe, G.D. Wilcox, J. Gonzalez-Garcia, F.C. Walsh, The rotating cylinder electrode: its continued development and application, J. Appl. Electrochem. 28 (1998) 759–780.
[9] G.W. Reade, C. Ponce-de-León, F.C. Walsh, Enhanced mass transport to a reticulated vitreous carbon rotating cylinder electrode using jet flow, Electrochim. Acta 51 (2006) 2728–2736.
[10] F.C. Walsh, A First Course in Electrochemical Engineering, Alresford Press, Alresford, 1993, p. 149 (Chapter 5).
[11] M. Eisenberg, C.W. Tobias, C.R. Wilke, Ionic mass transfer and concentration polarization at rotating electrodes, J. Electrochem. Soc. 101 (1954) 306–319.
[12] J.M. Grau, J.M. Bisang, Electrochemical removal of cadmium from dilute aqueous solutions using a rotating cylinder electrode of wedge wire screens, J. Appl. Electrochem. 37 (2007) 275–282.
[13] A.H. Nahlé, G.W. Reade, F.C. Walsh, Mass transport to reticulated vitreous carbon rotating cylinder electrodes, J. Appl. Electrochem. 25 (1995) 450–455.
[14] J.M. Grau, J.M. Bisang, Mass transfer studies at rotating cylinder electrodes of expanded metal, J. Appl. Electrochem. 35 (2005) 285–291.
[15] J.M. Grau, J.M. Bisang, Mass transfer studies at packed bed rotating cylinder electrodes of woven-wire meshes, J. Appl. Electrochem. 36 (2006) 759–763.